

Analytical model of nanowire FETs in a partially ballistic or dissipative transport regime

Paolo Michetti, Giorgio Mugnaini, Giuseppe Iannaccone *Member, IEEE*,

Abstract—The intermediate transport regime in nanoscale transistors between the fully ballistic case and the quasi-equilibrium case described by the drift-diffusion model is still an open modeling issue. Analytical approaches to the problem have been proposed, based on the introduction of a backscattering coefficient, or numerical approaches consisting in the Monte Carlo solution of the Boltzmann transport equation or in the introduction of dissipation in quantum transport descriptions. In this paper we propose a very simple analytical model to seamlessly cover the whole range of transport regimes in generic quasi-one dimensional field-effect transistors, and apply it to silicon nanowire transistors. The model is based on describing a generic transistor as a chain of ballistic nanowire transistors in series, or as the series of a ballistic transistor and a drift-diffusion transistor operating in the triode region. As an additional result, we find a relation between the mobility and the mean free path, that has deep consequences on the understanding of transport in nanoscale devices.

Index Terms—nanowire transistors, quantum wires, one-dimensional transistors, ballistic transport, compact model, drift-diffusion transport

I. INTRODUCTION

Multiple gate architectures such as gate-all-around (GAA) MOSFETs have lately attracted significant interest [1], [2], [3], and have emerged as promising options to keep short channel effects under control, exhibiting quasi-ideal subthreshold swing with undoped channels. This has the very important consequence of alleviating intrinsic variability of transistor threshold voltage, which in planar MOSFETs is mainly due to channel doping.

Nanowire FETs are a particular case of multiple gate FETs, in which quantum confinement occurs in the transverse cross section of only few nanometers. Nanowire FETs are basically quasi one-dimensional transistors, where transport occurs in a set of loosely coupled propagating modes.

From the point of view of modeling, several papers have appeared in the literature addressing transport and quantum confinement in silicon nanowire transistors. In pioneering works [4], [5], [6], [7], the effects of quantum confinement on a silicon nanowire were discussed. Numerical detailed investigations of quantum confinement in silicon and silicon

germanium nanowires with the anisotropic effective mass approximation, and its effect in lifting the degeneracy of silicon conduction band minima were discussed in [8], [9]. The electrostatics of silicon nanowire devices with cylindrical symmetry has been investigated through a perturbative approach to the Schrödinger equation [10] or with a self-consistent solution in Poisson-Schrödinger equation with cylindrical coordinates [11].

Analytical models of ballistic nanowire transistors have been proposed in [12], [13], [14] and a broad review can be found in [15]. In real nanowire devices currents are much lower than those predicted by ballistic models [2], which can only be used as an asymptotic performance limit.

Non ballistic transport in quasi-1D channels is harder to model. As far as numerical studies are concerned, far-from-equilibrium transport in silicon nanowire transistors was investigated in [16] within the non-equilibrium Green's functions formalism, for both ballistic and dissipative transport, using the Büttiker probes approach to model inelastic scattering. A subband-based drift-diffusion simulation, in which the 3D electrostatics is solved self-consistently with the 2D Schrödinger equation in each transverse cross section and a set of 1D continuity equations based on the drift-diffusion description, has been proposed in [17].

As far as analytical models of dissipative transport in quasi-1D FETs are concerned, notable examples are Ref. [13], which proposed a semiclassical model with drift-diffusion transport and constant mobility inside a cylindrical MOSFET, and Ref. [18], in which a polynomial expansion of the Fermi integrals for the mobile charge is used.

Specific scattering mechanisms such as phonon scattering have been numerically addressed within the non-equilibrium Green's functions approach by Jin *et al.* [19] and by M. Gilbert *et al.* [20], [21].

We believe it would be very interesting to have an analytical model capable to seamlessly cover the continuum of transport regimes between the limits of ballistic transport and drift-diffusion (i.e. quasi-equilibrium) transport. Such a model, theoretically derived from the formalism of Büttiker virtual probes [22], and consisting in either a chain of ballistic transistors or in the series of a fully ballistic and an ideal drift-diffusion transistor, has been proposed in [23], [24] for 2D MOSFETs.

On the basis of this work, in the present paper we present an analytical model capable of describing the complete range of transport regimes in quasi-1D FETs, from fully ballistic to long channel quasi-equilibrium drift-diffusion behavior. A preliminary attempt has been proposed in [25]. As we shall

This work was supported in part by the EC Nanosil FP7 Network of Excellence under Contract 216171 and in part by the European Science Foundation EUROCORES Programme Fundamentals of Nanoelectronics, through fundings from Consiglio Nazionale delle Ricerche (awarded to IEEIIT-PISA) and the European Commission Sixth Framework Programme under Project Dewint (Contract ERAS-CT-2003-980409).

Authors are with the Dipartimento di Ingegneria dell'Informazione, Università di Pisa, Pisa I-56122, Italy (e-mail: p.michetti@iet.unipi.it; g.iannaccone@iet.unipi.it).

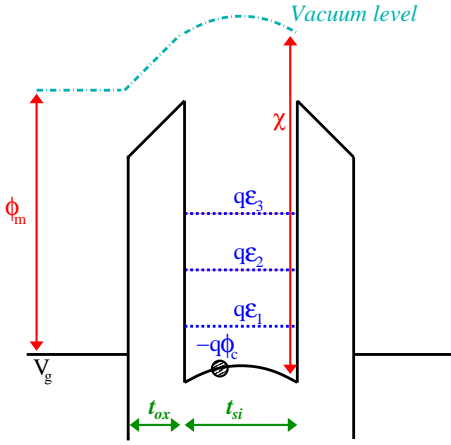


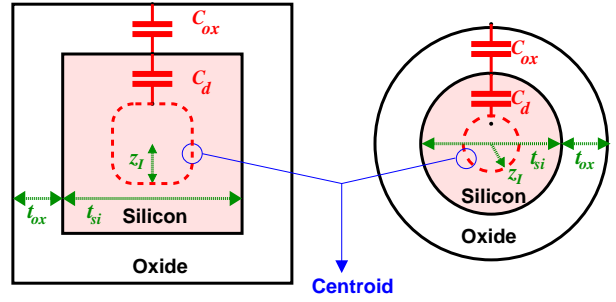
Fig. 1. Schematic band diagram of a 1D SNWT. V_g is the gate Fermi potential, ϕ_m is the gate workfunction, χ is the channel electron affinity, ϕ_c is the potential in the centroid layer. $q\epsilon_\alpha$ are the eigenvalues of the vertical confinement, drawn out of scale.

show, the model is sufficiently simple to be suitable for circuit-level simulations and provides a strong intuitive picture of the transition from ballistic to drift-diffusion transport, which is missing in other descriptions of partially ballistic transport such as those relying on the introduction of a backscattering coefficient [26], [27].

The paper is organized as follows: in Section II we set up a model for ballistic transport in a nanowire transistor, that, in Section III, we apply to the case of a chain of ballistic transistors. With a linearization procedure we show that a sufficiently long chain of ballistic transistors, can be regarded as a drift-diffusion channel. But the same approach fails for short ballistic chains, in which transport has an intermediate nature between ballistic and drift-diffusion. This difficulty is tackled in Section IV, where we present a compact model for intermediate transport that treats the ballistic chain as a series of one drift-diffusion section, for the first $N - 1$ transistors, and the remaining one ballistic channel, in which the non-equilibrium character of the intermediate transport manifests itself. In Section V we introduce the cylindrical and rectangular confinements for silicon nanowires considered in this paper and in Section VI we compare the results of our drift-diffusion and intermediate transport compact models with the numerical solution of the transport through ballistic chains of different length. In the section we also give an estimation of the current ballisticity ratio as a function of the transistor chain length.

II. BALLISTIC TRANSPORT

In the following discussion, we describe our approach in the general situation of a n-FET with a quasi-1D channel, with the effective mass approximation. Indeed the subband energies are determined by the transverse confinement, and to explicitly account for the capacitive coupling between gate and channel, the contact geometry has to be taken in account. The bottom of the 1D conduction subbands are formally defined as the sum $q\epsilon_\alpha - q\phi_c$, of the eigenstates of the vertical confinement with respect to the conduction band edge in the



	t_{si}	t_{ox}	z_I
R	4 nm	3 nm	0.97 nm
C	4 nm	3 nm	0.92 nm

Fig. 2. Schematic capacitance diagram for a wire with square and circular cross section, representing the series of the oxide capacitance C_{ox} and the silicon capacitance C_d . In the square shape the interface between the silicon and the insulator is considered approximately isopotential and the mobile charge layer (the centroid z_I) is approximated with a square contour. The table summarizes the geometrical parameters used in the simulation of the rectangular wire (R) and cylindrical one (C).

centroid layer ($q\epsilon_\alpha$) and of the electrostatic potential energy ($-q\phi_c$) in the centroid layer, that is where one can think all charge localized, following the approach of Refs. [28], [23]. For simplicity, α denotes the set of the quantum numbers specifying the confinement. The dimensionality also modifies the Fermi-Dirac integrals $F_{\nu-1/2}$ and F_ν entering the ballistic equations for the mobile charge and the current in the channel, respectively. In particular for a 1D conductor, in effective mass approximation, $\nu = 0$, whereas for a 2D MOSFET $\nu = 1/2$ [24]. A definition for the Fermi integrals, with $\nu > -1$, is

$$F_\nu(\eta) = \frac{1}{\Gamma(\nu+1)} \int_0^\infty \frac{x^\nu}{e^{x-\eta} + 1} dx \quad (1)$$

with Γ being the Gamma function, acting as a normalizing factor for the Fermi integrals. For $\nu \leq -1$ we can rely to their property $(d/d\eta)F_\nu(\eta) = F_{\nu-1}(\eta)$ for their definition [29].

We start from a generic multi-subband degenerate version of the ballistic model in [24]. The vertical electrostatic model we propose, is similar to that in [12], [13], it is also somewhat less sophisticated, because we will suppose that screening can be considered constant. This is done in view of obtaining an analytical model of intermediate transport. Anyway we note that this assumption is sound enough for small cross-section channels and low electron densities [30]. Indeed, in the inverse layer centroid approach, we consider the charge accumulated in the centroid layer and its geometrical screening is included in the effective gate capacitance as a series contribution C_d , therefore the effective gate oxide capacitance for unit length is given by:

$$C_g = \left(\frac{1}{C_{ox}} + \frac{1}{C_d} \right)^{-1} \quad (2)$$

as reported in Figure 2, where the expression C_{ox} depends on the geometry.

If we suppose an undoped channel, consistently with Fig.1, the linear density of mobile charge on the peak of the potential

barrier in the channel is given by:

$$Q_m = -C_g [V_g - (\phi_m - \chi)/q - \phi_c], \quad (3)$$

where ϕ_c is the electrostatic potential in the centroid layer, $(\phi_m - \chi)/q$ is the flat band potential, given by the difference between the gate workfunction ϕ_m and the channel electron affinity χ .

In the case of ballistic transport, there is no local equilibrium so that no quasi-Fermi level can be locally defined, because two different carrier populations exist, originating from source and drain, that can be considered at equilibrium with the injecting electrodes, as discussed in [31]. These two populations are separated by the peak of the barrier in the channel, that controls transport. Therefore, only three points are important: source, drain and the peak of the electrostatic potential. In ballistic transport, carriers move without inelastic scattering along the channel and therefore at the subband peak the carriers that propagate toward the drain (“forward states”) only come from the source, whereas the carriers propagating toward the source (“reverse” states) come from the drain. As a consequence, we have the superposition of two hemi-Fermi-Dirac distributions. Following the considerations in [12], we can write for the ballistic mobile charge linear density on the peak:

$$Q_m = -q \sum_{\alpha} N_{\alpha} [F_{-1/2}(\eta_s^{\alpha}) + F_{-1/2}(\eta_d^{\alpha})], \quad (4)$$

where:

$$N_{\alpha} = g_{\alpha} \sqrt{\frac{k_B T m_{\alpha}}{2\pi^2 \hbar^2}} \Gamma\left(\frac{1}{2}\right)$$

is one half of the effective density of states of the α -th subbands multiplied for its degeneration index g_{α} . $F_{-1/2}(\eta)$ is the Fermi integral of order $-1/2$ and

$$\begin{aligned} \eta_s^{\alpha} &= (\phi_c - V_s - \varepsilon_{\alpha})/\phi_t, \\ \eta_d^{\alpha} &= (\phi_c - V_d - \varepsilon_{\alpha})/\phi_t. \end{aligned} \quad (5)$$

The Fermi potential at the source (drain) is $V_{s(d)}$ and $\phi_t = K_b T/q$ is the thermal potential. Equations (3) and (4) have to be solved simultaneously to obtain ϕ_c and Q_m .

From the Landauer formula, we can write the current as [12]:

$$I_{ds} = q \sum_{\alpha} G_{\alpha} [F_0(\eta_s^{\alpha}) - F_0(\eta_d^{\alpha})], \quad (6)$$

where $G_{\alpha} = g_{\alpha} \frac{k_B T}{\pi \hbar} \Gamma(1)$ is the effective injection rate of a 1D channel multiplied by the degeneration g_{α} of the α -th subband. Note that the current is dependent on the channel potential through η_s and η_d .

III. FROM BALLISTIC TO DRIFT-DIFFUSION TRANSPORT

We follow the approach developed in [23], [24] for a 2D MOSFET for the non-degenerate and degenerate cases. Here we analyze the case of a silicon nanowire transistor (SNWT) where the different dimensionality leads to different Fermi integrals entering the current and the charge expressions, and to different electrostatics. Moreover we considered a multi-subband degenerate model while in [24] only a single subband was presented. We obtain also a correcting factor for the

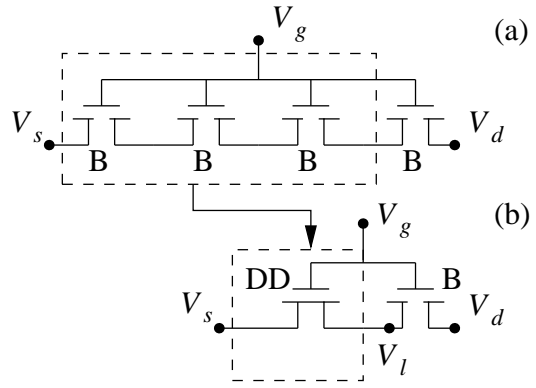


Fig. 3. (a) Circuit model of a generic SNWT, subject to inelastic scattering, in terms of a convenient chain of ballistic (B) SNWTs. (b) Approximate aggregation of the first $N - 1$ ballistic transistors in an equivalent Drift-Diffusion (DD) one. The macromodel DD+B comes out to be a suitable model for a device in intermediate transport regime.

degenerate case, correcting the result of the linearization process whenever the low field approximation is not in fully satisfied.

We recall that, within the Büttiker probes approach, inelastic scattering is thought as localized in special points, spaced by a length defined as “mean-free path” λ . The virtual probes act as localized reservoirs along the channel, in which carriers are thermalized in equilibrium with their quasi-Fermi potential V_k , while transport from one virtual probe to the next is considered purely ballistic. We have a drift-diffusion transistor when the channel length is much longer than the free mean path, that from our point of view it is equivalent to have a long enough chain of ballistic transistors, as rigorously shown in [23]. On the contrary, when the number of internal contacts is small, transport is far-from-equilibrium, and is fully ballistic in the limit $N = 1$. We remark that within the Büttiker probe approach, transport of hot electrons is accounted only inside each ballistic channel, whereas a full thermalization occurs in correspondence of each probe, where electron density is described by a single quasi-Fermi level. It would also be interesting, but out of the scope of the present paper, to couple the transport equation with a heat diffusion equation, accounting for the energy losses in the Büttiker probes, leading to a non uniform temperature distribution in the device.

We define V_k as the quasi-Fermi potential of the k -th virtual probe, and suppose that the k -th contact is placed at $x_k = k\lambda$ with $k = 1, \dots, N$, where the boundaries are fixed as $V_0 = V_s = 0$ V and $V_N = V_d = V_{ds}$. That is equivalent to place N ballistic SNWTs of channel length λ in series, as sketched in Figure 3. Since the current I_k in any $k = 1, \dots, N$ FET must be equal to I_{ds} , we have N equations determining the local Fermi levels:

$$I_k = q \sum_{\alpha} G_{\alpha} [F_0(\eta_{k-1}^{\alpha}) - F_0(\eta_k^{\alpha})]. \quad (7)$$

We note that $\eta_k^{\alpha} = (\tilde{\phi}_k - V_k - \varepsilon_{\alpha})/\phi_t$ where $\tilde{\phi}_k$ is the electrostatic self consistent potential in the conduction band peak of channel k , between the source contact $k - 1$ and the drain contact k . Introducing the definition $\tilde{V}_k \equiv (V_{k-1} + V_k)/2$, i.e. the mean potential between the two contacts (k and $k - 1$)

of channel k , and making explicit the Fermi integrals, we can rearrange (7) as follows

$$I_k = q \sum_{\alpha} G_{\alpha} \int_0^{\infty} \frac{\sinh\left(\frac{V_k - V_{k-1}}{2\phi_t}\right)}{2 \left[\cosh\left(\frac{x - \tilde{\eta}_k^{\alpha}}{2}\right) \right]^2 + \left[\cosh\left(\frac{V_k - V_{k-1}}{2\phi_t}\right) - 1 \right]} dx \quad (8)$$

where $\tilde{\eta}_k^{\alpha} = (\tilde{\phi}_k - \tilde{V}_k - \varepsilon_{\alpha})/\phi_t$.

At this point, in order to build an analytical model, we consider a large number of contacts and, having in mind that the current is constant along the channel, we extend V_k to a continuous quasi-Fermi potential $V(x)$ satisfying the conditions:

$$V\left(\frac{x_k + x_{k-1}}{2}\right) = \tilde{V}_k \quad (9)$$

$$\frac{dV}{dx}\left(\frac{x_k + x_{k-1}}{2}\right) = \frac{V_k - V_{k-1}}{\lambda}. \quad (10)$$

Under the particular hypothesis that every ballistic SNWT works in the linear region i.e. that:

$$\lambda \frac{dV(x)}{dx} = V_k - V_{k-1} \ll 2\phi_t, \quad (11)$$

and expanding the terms \sinh and \cosh to the first order, we can put (8) in the local form

$$I = \frac{q\lambda}{\phi_t} \frac{dV(x)}{dx} \sum_{\alpha} G_{\alpha} F_{-1}[\eta^{\alpha}(x)] \quad (12)$$

where the quantities pertain to the point x , as

$$\eta^{\alpha}(x) = [\phi(x) - V(x) - \varepsilon_{\alpha}]/\phi_t. \quad (13)$$

Evidently, if a voltage V_{ds} is applied to the chain, (11) is satisfied if $V_{ds} \ll 2\phi_t N$. Moreover, within the same approximations, the vertical electrostatics becomes:

$$Q(x) = \sum_{\alpha} Q^{\alpha}(x) = 2q \sum_{\alpha} N_{\alpha} F_{-1/2}[\eta^{\alpha}(x)]. \quad (14)$$

An important aspect of (12) and (14) is that the current I^{α} in subband α can be written in terms of the mobile charge density $Q^{\alpha}(x)$ and of a mobility $\mu_{deg}^{\alpha}(x)$ as:

$$I^{\alpha}(x) = \mu_{deg}^{\alpha}(x) Q^{\alpha}(x) \frac{dV(x)}{dx} \quad (15)$$

where the conduction is affected by the 1D electron gas degeneracy through the mobility $\mu_{deg}^{\alpha}(x)$. The mobility is given by

$$\mu_{deg}^{\alpha}(x) = \frac{v_{\alpha} \lambda}{2\phi_t} \frac{F_{-1}[\eta^{\alpha}(x)]}{F_{-1/2}[\eta^{\alpha}(x)]} \quad (16)$$

where $v_{\alpha} \lambda / 2\phi_t$, to which the expression (16) is reduced in the non-degenerate limit, represents the low-field mobility for a 1D gas of incoming electrons described by an hemi Maxwell-Boltzmann statistics [24] occupying the α -th subband, whose mean electron velocity is $v_{\alpha} = \sqrt{\frac{2kT}{\pi m_{\alpha}}}$, characterized by a ballistic motion for paths of length $l < \lambda$ and a sudden and complete scattering at $l = \lambda$. Considering the mean free path λ as a constant, (16) describes the degradation of carrier mobility due to degenerate conditions of Fermi-Dirac statistics. An analogous expression was recognized in a Monte Carlo simulation [32] for the case of strained silicon FETs. While,

in [16] and [27], a similar, but not identical relation between the mean free path and the effective mobility has been found.

The current is expressed in a local form in (12) and we can eliminate the gradient of the local quasi-Fermi level integrating along the channel and exploiting current continuity, leading to

$$I_{ds} = \int_0^L q \frac{\lambda}{\phi_t L} \sum_{\alpha} G_{\alpha} F_{-1}[\eta^{\alpha}(x)] \frac{dV(x)}{dx} dx. \quad (17)$$

In order to obtain a more compact form of (17), we can change the integral variable as follows

$$\int_0^L q F_{-1}[\eta(x)] \frac{dV(x)}{dx} dx = \int_{V_s}^{V_d} F_{-1}[\eta(V)] dV = \int_{\eta_s}^{\eta_d} F_{-1}(\eta) \frac{dV}{d\eta} d\eta, \quad (18)$$

where the term $dV/d\eta$ is obtained by differentiating (14) in dV and using the fact that $d\eta/dV = (d\phi/dV - 1)/\phi_t$. The current can be obtained with a numerical integration of

$$I_{ds}^{\alpha} = \frac{q\lambda G_{\alpha}}{\phi_t L} \int_{V_s}^{V_d} F_{-1}[\eta_{\alpha}(V)] dV, \quad (19)$$

where we note that η_{α} not only explicitly depends on V , but also implicitly through ϕ_c , as shown in (13). Such dependence has to be taken into account in the self-consistent solution of the vertical electrostatics.

Finally, we obtain the compact expression (which we will refer as the DD model) for the source-drain current for each subband α

$$I_{ds}^{\alpha} = \frac{q\lambda\phi_c G_{\alpha}}{\phi_t L} \left([F_0(\eta_s^{\alpha}) - F_0(\eta_d^{\alpha})] + \sum_{\beta} \rho_{\beta} [\mathcal{F}_{-1,-3/2}(\eta_s^{\alpha}, \eta_s^{\beta}) - \mathcal{F}_{-1,-3/2}(\eta_d^{\alpha}, \eta_d^{\beta})] \right). \quad (20)$$

Where for simplicity we defined

$$\mathcal{F}_{-1,-3/2}(\eta^{\alpha}, \eta^{\beta}) \equiv \int_{-\infty}^{\eta^{\alpha}} F_{-1}(x) F_{-3/2}\left(x + \frac{\varepsilon_{\beta} - \varepsilon_{\alpha}}{\phi_t}\right) dx, \quad (21)$$

with $\rho_{\alpha} = \frac{qN_{\alpha}}{C_g\phi_c}$. It is worth noting that, as observed also in [23], [24], in the non-degenerate limit the first term in (20) reduces to the diffusion term of the EKV model, while in the degenerate limit, it corresponds to the current of a single ballistic channel divided by N . The second term of (20) is instead associated with the drift current.

We note that actually, in the low field approximation, for the case of a 1D channel, the integral (8) can be analytically solved as discussed in Appendix I. However, the use of the analytical expression leads to the more complex and numerically expensive expression for the drift-diffusion current (29), while giving only a slight correction of (19). The model that employs the analytical solution of (8), with the use of (29), will be referred as DD* model. We conclude stressing the fact that DD and DD* models, considered alone, are not appropriate to describe transport whenever the condition (11) is not satisfied: for example in very short channels, where intermediate transport is expected.

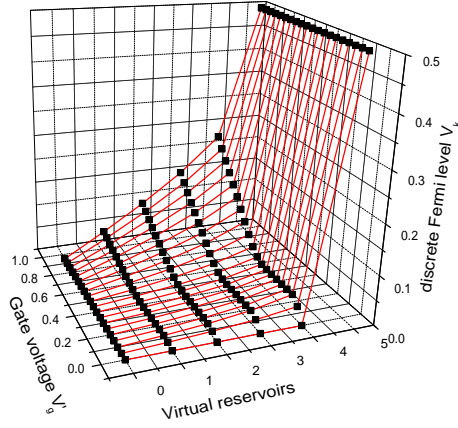


Fig. 4. Discrete quasi-Fermi potential for a chain of $N = 5$ SNWTs at fixed $V_{ds} = 0.5$ V. Fermi level is defined only on the virtual probes placed at points $x = k\lambda$ with $k = 1 \dots N$. It is evident that the first $N - 1$ transistors work approximately in linear regime, while increasing V_g a non-linear behavior is

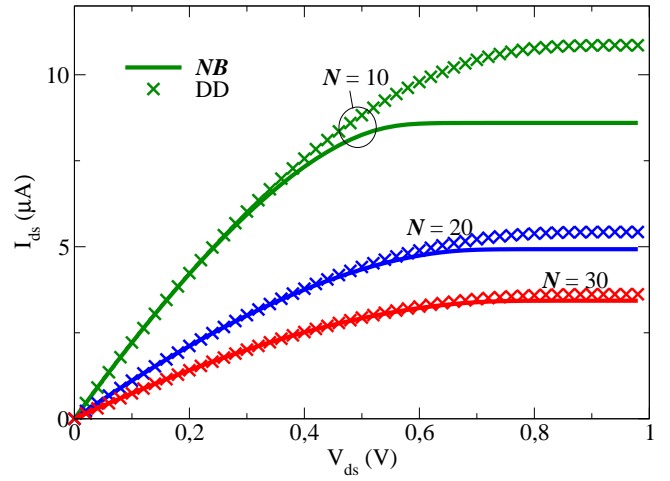


Fig. 6. Output characteristics for a chain of N ballistic cylindrical C SNWTs (denoted by NB), for $N = 10, 20, 30$, compared with results of the DD model with $\lambda = L/N$. The gate potential value is $V_g = 0.8$ V. As the number of ballistic transistors in series increases the drift-diffusion approximation become more and more able to capture the behavior of the device.

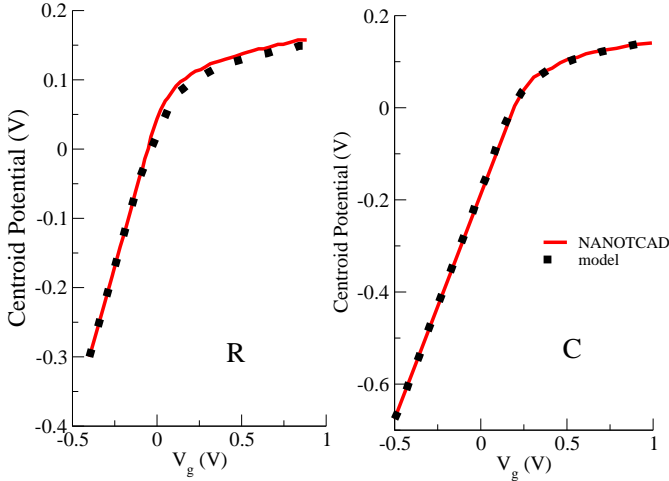


Fig. 5. Comparison between NANOTCAD 2D simulation and the compact model calculation of the vertical electrostatic for the R and C SNWTs. The centroid potential obtained with NANOTCAD 2D (solid line) and the centroid potential obtained with the compact model (dotted) are reported. The compact model well accounts for the centroid potential, point in which the charge of the channel can be thought to be concentrated.

IV. COMPACT MODEL FOR INTERMEDIATE TRANSPORT

Now we are interested in the development of a model that will be effective in the whole range of transport regimes, as proposed in [23] for the 2D MOSFET case. It is evident that in the general case of intermediate transport, the simplifying hypothesis (11), that enforces each SNWT of the ballistic chain to operate in the linear region, does not hold, and we can expect that some elementary channels can work in the saturation regime, or near it [23]. The behavior of a SNWT operating in such intermediate transport regime, can be obtained by solving the system for the complete ballistic chain (7), but it can represent a heavy computational burden, especially for a large number of internal nodes. In order to

build a simple model, that can be more easily handled, we note in Fig. 4, where we plotted the quasi Fermi potential on the virtual probes for a chain decomposition of a SNWT, that when the saturating behavior of the elementary ballistic transistor emerges, it is present mainly on the last ballistic transistor of the chain. This non-linear behavior is a general condition for transistors in intermediate transport regime, due to the fact that in its end the channel narrows down and therefore, to maintain constant the current flux along it, a major spacing between the last source and drain levels is required (or, in the continuous limit, a steep drop of the quasi Fermi level). This fact suggests that we can aggregate the first $N - 1$ ballistic transistors in an approximate equivalent drift-diffusion transistor with ratio $L/\lambda = N - 1$ working in low field conditions, as it is represented in Fig. 3, and similarly to what was proposed in [23] for MOSFETs. We can therefore see a SNWT in intermediate regime as the series of a drift-diffusion (DD) channel for the first $N - 1$ transistor, that we can solve using (19), and a single ballistic transistor, governed by (6). We only need to solve the DD+B system, imposing constant current through the two sections in series and solving the Fermi potential on the internal node between the DD and the B channels. We point out that in the DD+B model the ratio L/λ has no need to be integer, because we apply the continuous DD equation (20).

V. APPLICATION TO GAA-SILICON NANOWIRE

At first we will consider a silicon wire with square cross section of side t_{si} . Concerning the effective gate capacitance, unfortunately no simple analytical closed form is available. In order to simplify the electrostatics, we suppose that the interface between the oxide and silicon is approximately isopotential and we consider the variational approximation reported in [33], where the capacitance per unit length of a

rectangular coaxial line, associated with the oxide layer, is

$$C_{ox} = \frac{8\epsilon_{ox}}{\ln\left(1 + \frac{t_{ox}}{t_{si}}\right)} \quad (22)$$

and similarly the capacitance associated with the charge in the silicon body C_d is

$$C_d = \frac{8\pi\epsilon_{si}}{\ln\left(\frac{t_{si}}{2z_l}\right)}. \quad (23)$$

The use of C_d , with z_l adequately chosen, permits to treat the capacitance due to the charge distribution in the channel cross section, in series with the oxide capacitance C_{ox} . The term z_l is a characteristic dimension of the closed line where we can effectively localize the whole mobile charge. Here it is used as a fitting parameter for simplicity, while it is actually dependent, due to volume inversion, on the charge density in the channel. We point out though that it is smoothly varying for small section nanowires and low electron density [30].

In case of rectangular quantum confinement, the eigenvalues of the Schrödinger equation can be considered for simplicity [12]:

$$q\epsilon_{n_x, n_y}^{\nu} = \frac{\hbar^2 \pi^2}{2} \left[\frac{n_x^2}{m_x^{\nu} t_{si}^2} + \frac{n_y^2}{m_y^{\nu} t_{si}^2} \right], \quad (24)$$

where the mass tensor can be defined as:

ν	m_x^{ν}	m_y^{ν}	m_z^{ν}
1	m_l	m_l	m_t
2	m_l	m_t	m_t
3	m_t	m_t	m_l

m_l and m_t are the longitudinal and transverse components of the effective mass tensor of the degenerate minima of the conduction bands in Si. We can write the effective mass, characterizing the motion in the unconfined direction (z), as $m_{\nu} = m_z^{\nu}$ for a (100) silicon wire, with ν running on the different Si conduction band minima.

In the case of cylindrical quantum confinement, for the gate capacitance, we have instead:

$$C_{ox} = \frac{2\pi\epsilon_{ox}}{\ln\left(1 + \frac{t_{ox}}{t_{si}}\right)} \quad (25)$$

and

$$C_d = \frac{2\pi\epsilon_{si}}{\ln\left(\frac{t_{si}}{2z_l}\right)}. \quad (26)$$

Considering cylindrical quantum confinement [12], we have that the subband separation from the bottom of the conduction band is described by the approximated and handy expression:

$$q\epsilon_{n_1, n_2}^{\nu} \approx \frac{\hbar^2 \pi^2}{2 \sqrt{m_x^{\nu} m_y^{\nu}} R^2} \left(n_1 + |n_2| - \frac{1}{4} \right)^2 \quad (27)$$

where n_1 is the radial quantum number, n_2 the azimuthal quantum number and ν runs on the different silicon valleys.

We applied our model to a cylindrical quantum wire and a rectangular SNWT, denominated C , R respectively. Their geometries are described by Fig. 2. The inversion centroid layer depth was fixed in comparison with the 2D Schrodinger-Poisson simulator NANOTCAD [34], as shown in Fig. 5.

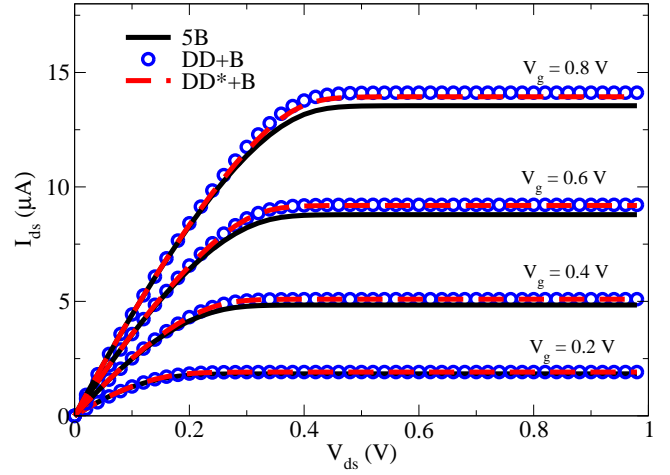


Fig. 7. Output characteristics of a C SNWT modeled as a chain of $N = 5$ elementary transistors: 5B corresponds to the exact numerical evaluation. The DD+B compact model is obtained considering the series of a DD channel governed by (20) plus a ballistic one and the DD*+B is analogous but uses (29) for the DD section. The choices of the gate potential are $V_g = 0.2, 0.4,$

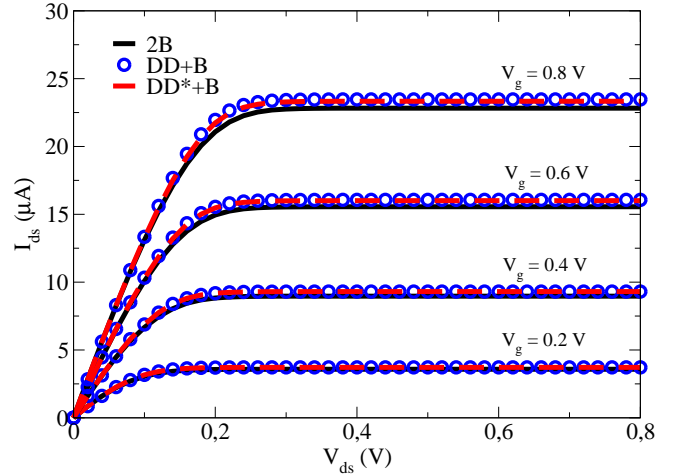


Fig. 8. Output characteristics of the R SNWT modeled as a chain of $N = 2$ elementary transistors: exact numerical evaluation (2B), compact model DD+B with a drift-diffusion plus a ballistic channels and DD*+B analogous to the latter except for the use of (29) in the DD section. The choices of the gate potential are $V_g = 0.2, 0.4, 0.6, 0.8$ V.

We note that a careful choice of z_l permits to recover the inverse layer centroid potential in full agreement with the NANOTCAD simulator, correctly accounting, thus, for the screening due to the charge inside the channel as a function of the gate potential.

VI. RESULTS

For a short channel transistor with length of few mean free paths, transport is quasi ballistic, and we have seen that the DD model (19) fails to describe its behavior. On the other hand, it is well known that the transport regime of a transistor with channel length much longer than the free mean path is described by the drift-diffusion model. We want to check if our model is able to correctly reproduce such transition and to investigate the number of free mean paths after which transport

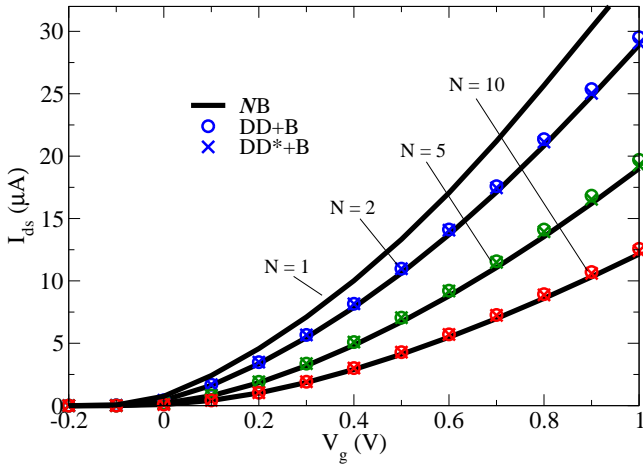


Fig. 9. Transcharacteristic curves for a chain of N ballistic C SNWTs, with N ranging from 1 to 10 and $V_{ds} = 0.5$ V. The exact numerical evaluation (NB), and the results of the DD+B and DD*+B compact models are shown.

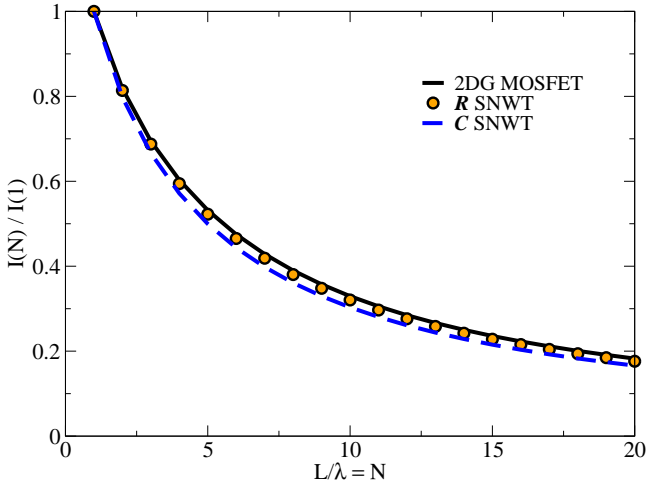


Fig. 10. Ballistic index of a NB chain as a function of N for the R, C SNWTs, and a MOSFET (see text for details). The gate potential is $V_g = 0.8$ V and the drain-source potential is $V_{ds} = 0.5$ V.

can be definitely associated to the drift-diffusion regime. In Fig.6 we plot the output characteristics for a chain of N ballistic channels numerically calculated (denoted NB) and with the Drift-Diffusion approximation (DD characteristics), for $N = 10, 20, 30$ and gate potential $V_g = 0.8$ V. We note that for a SNWT of length smaller than 10λ , a DD description is not appropriate. With increasing N the difference between the NB and DD models is reduced, and for a channel of length $> 20\lambda$ the output characteristics calculated with the DD model fully reproduce the corresponding numerically evaluated NBs.

We have calculated the output characteristics of SWNTs described in the latter section employing a direct numerical solution of the chain of N ballistic transistors (NB), and compared them with our models for intermediate transport DD+B and DD*+B. Figure 7 and 8 respectively show the output characteristics for the C SWNT with $N = L/\lambda = 5$, and for the rectangular SWNT with $N = 2$. Similar considerations apply to the two figures. While the DD approximated equation, derived from the linearization of the NB chain, inadequately

reproduces the saturation behavior of the NB characteristics, the DD+B model seems suitable to describe SNWTs in the intermediate transport regime. As shown in 7 and 8 the DD+B and DD*+B models are really able to capture the non-linear behavior of the NB transistors, although a non negligible error remains in the saturation regime. This is due to the the weakly non-linear transport in the DD section, that has been neglected. We note that in general the DD+B* improves the agreement with the ballistic chain characteristics.

After testing our model with rectangular and cylindrical nanowire geometries, changing both the oxide and silicon length t_{ox}, t_{si} and with different values of N , we can conclude that the DD+B and DD*+B compact model quite well reproduces the output characteristics of degenerate SWNTs for any N , with errors in the saturation zone of few percentage points.

In Fig. 9 the transfer characteristics of a C SNWT, treated as a chain of N elementary ballistic channels, with $V_{ds} = 0.5$ V, is presented. Both the DD+B and the DD*+B models well reproduce the behavior of the corresponding ballistic chain in all gate voltage regimes, for all values of N . We note that the DD*+B model is always more accurate, in particular the correction is more evident for transistor with few nodes, at large gate voltage.

We investigated also the so called ballisticity index of a transistor [35], that is given by the current ratio I/I_b , between the current of the transistor and that of a corresponding ballistic one. The results of its calculation for a NB chain, with N ranging from 1 to 20, are shown in Fig.10, where we considered the R, C SNWTs and also, for comparison an undoped Double Gate MOSFET with $t_{si} = 4$ nm, $t_{ox} = 2$ nm. The ballisticity index is monotonous and slowly decaying with N , the behavior is similar for all the transistors considered here. The curves can be easily fitted with the function $1/[1 + r(N - 1)]$ where N is the number of ballistic elements and $r \approx 0.25$. We note that initially the ballisticity index steeply decreases with N . For longer channels the current becomes slowly varying with N : sliding from $N = 10$ to $N = 20$ the current only decreases from the 30% to the 20% of the ideal ballistic one.

Having in mind a compact model, the calculation of equations (20) or (19) for the DD+B model are still computationally expensive. Therefore we also tested the approximation of the integral in the drift-diffusion section (DD) with its symmetrical linearization [36], as discussed in Appendix II.

VII. CONCLUSION

We have presented a physics-based analytical model able to describe quasi one-dimensional field-effect transistors in the complete range of transport regimes extending from the fully ballistic case captured by the Natori model to the quasi-equilibrium case captured by the drift-diffusion description. Our proposed model sees a generic transistor as a long enough chain of elementary ballistic transistors in series with a common gate. Based on the Büttiker probes description of inelastic scattering, we have rigorously proved that the model reduces to the limit cases. In addition, as the most important result in this paper, we have shown that an equally adequate

model, much simpler from the computational point of view, and more physically intuitive, is represented by the series of an appropriate drift-diffusion one-dimensional transistor and a ballistic one-dimensional transistor, consistently with the results in [23], [24], that apply to 2DEG FETs. We have focused in this paper on silicon nanowire transistors, but our model is applicable without significant variations to any type of quasi-one dimensional FET, such as those based on carbon nanotubes, graphene nanoribbons, or other channel materials.

Finally, we have shown that an interesting consequence of our model is that, if a uniformly spaced chain is assumed, the Fermi-Dirac statistics degrades the low-field mobility, consistently with the observations in [32].

APPENDIX I

ANALYTICAL SOLUTION OF THE DD INTEGRAL

We note that in the integral

$$\int_0^{\infty} \frac{1}{2 \left[\cosh\left(\frac{x-\tilde{\eta}^\alpha}{2}\right) \right]^2 + \left[\cosh\left(\frac{V_k-V_{k-1}}{2\phi_t}\right) - 1 \right]} dx,$$

in (8) has an analytical solution given by

$$I(\tilde{\eta}) = \frac{1}{\sqrt{a(a+1)}} \times \left\{ \tanh^{-1} \left[\sqrt{\frac{a}{a+1}} \right] + \tanh^{-1} \left[\sqrt{\frac{a}{a+1}} \tanh\left(\frac{\tilde{\eta}^\alpha}{2}\right) \right] \right\},$$

where $a = \left[\cosh\left(\frac{V_k-V_{k-1}}{2\phi_t}\right) - 1 \right] / 2$. We replace the Fermi level difference between neighbor probes, by its mean value on the linearized chain

$$V_k - V_{k-1} \approx \gamma = \Delta V^{(DD)} / (2\phi_t N),$$

where $\Delta V^{(DD)}$ is the total potential drop in the DD section and N the number of elementary channels in it.

In the low-field approximation we also replaced the $\sinh\left(\frac{V_k-V_{k-1}}{2\phi_t}\right)$ with its arguments: we try to amend this by including a correction factor obtained by the ratio of the not-approximate term over approximate one

$$\sinh\left(\frac{V_k - V_{k-1}}{2\phi_t}\right) / \frac{V_k - V_{k-1}}{2\phi_t}. \quad (28)$$

In the end, we reach a more accurate version of (19) for the DD section, given by the following expression

$$I^\alpha = \frac{q\lambda G_\alpha}{\phi_t L} \frac{\sinh(\gamma)}{\gamma \sqrt{a(a+1)}} \int_{V_s}^{V_d} I[V] dV \quad (29)$$

APPENDIX II

SYMMETRICAL LINEARIZATION OF THE DD INTEGRAL IN SNWT

The integral for the drift-diffusion current (19) is computationally expensive for a compact model to be included in circuit simulators such as SPICE. Therefore we adopt a variant

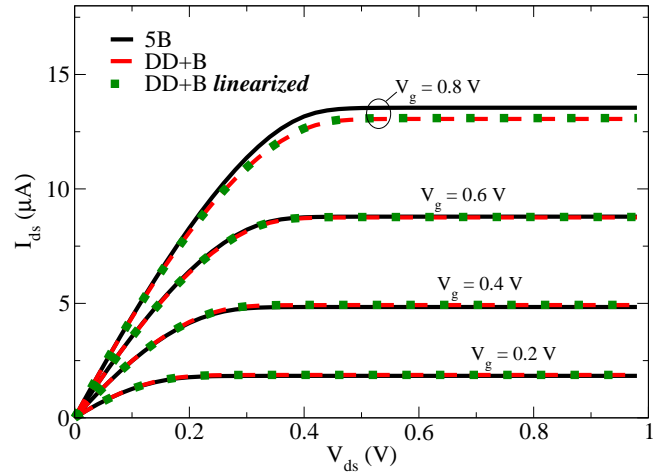


Fig. 11. Characteristic curves calculated for a R SNWT with $N = 5$. The results of the direct numerical calculation 5B, of the DD+B compact model and of the same compact model, employing symmetrical linearization DD_{lin}+B, discussed in the text, are shown. The curves are calculated for gate potential values of $V_g = 0.2, 0.4, 0.6, 0.8$ V.

of the symmetrical linearization [36], [37] in order to obtain an approximated result:

$$\begin{aligned} I &= \int_{V_s}^{V_d} q \sum_{\alpha} G_{\alpha} F_{-1}\left(\frac{\phi_c - V - \varepsilon_{\alpha}}{\phi_t}\right) \frac{dV}{dx} \frac{\lambda}{L} dx = \\ &= \int_{\phi_{cs}}^{\phi_{cd}} q \sum_{\alpha} G_{\alpha} F_{-1}\left(\frac{\phi_c - V - \varepsilon_{\alpha}}{\phi_t}\right) \frac{dV}{d\phi_c} \frac{\lambda}{L} d\phi_c = \\ &\approx q \sum_{\alpha} G_{\alpha} F_{-1}\left(\frac{\phi_{c,m} - V - \varepsilon_{\alpha}}{\phi_t}\right) \left(\frac{dV}{d\phi_c}\right)_m \frac{\lambda}{L} [\phi_{cd} - \phi_{cs}] = \\ &\approx q \frac{\lambda}{L} \sum_{\alpha} G_{\alpha} F_{-1}\left(\frac{\phi_{c,m} - V - \varepsilon_{\alpha}}{\phi_t}\right) [\phi_{cd} - \phi_{cs}] n_q \end{aligned}$$

where we have defined the “quantum slope factor”:

$$n_q \equiv 1 + \frac{1}{q \sum_{\alpha} \rho_{\alpha} F_{-\frac{3}{2}}\left(\frac{\phi_{c,m} - V_{c,m} - \varepsilon_{\alpha}}{\phi_t}\right)} \quad (30)$$

that is a constant in the considered case. The linearization is done around:

$$\phi_{c,m} = \frac{\phi_{cs} + \phi_{cd}}{2} \quad (31)$$

where ϕ_{cs} and ϕ_{cd} can be obtained solving the vertical electrostatics (14). Moreover from vertical electrostatics we find $V_{c,m}$ with an iterative process. We can observe in Fig.11 that the symmetrical linearization of the DD integral well reproduce the not-approximated results.

REFERENCES

- [1] L. Lauhon, M. Gudiksen, D. Wang, and C. Lieber, “Epitaxial core-shell and core-multishell nanowire heterostructures,” *Nature*, vol. 420, no. 6911, pp. 57–61, Nov. 2002.
- [2] N. Singh, A. Agarwal, L. Bera, T. Liow, R. Yang, S. Rustagi, C. Tung, R. Kumar, G. Lo, N. Balasubramanian, and D. Kwong, “High-performance fully depleted silicon nanowire (diameter ≤ 5 nm) gate-all-around cmos devoces,” *IEEE Electron Device Lett.*, vol. 27, no. 5, pp. 383–386, May 2006.

- [3] S. Suk, K. Yeo, K. Cho, M. Li, Y. Yeoh, S. Lee, S. Kim, E. Yoon, M. Kim, C. Oh, S. Kim, D. Kim, and D. Park, "High-performance twin silicon nanowire mosfet (tsnwfet) on bulk si wafer," *IEEE Trans. Manotechnol.*, vol. 7, no. 2, pp. 181–184, Mar. 2008.
- [4] G. Sanders, C. STANTON, and Y. CHANG, "Theory of transport in silicon quantum wires," *Phys. Rev. B*, vol. 48, no. 15, p. 11067, Oct. 1993.
- [5] M. Shen and S. Zhang, "Band-gap of a silicon quantum-wire," *Phys. Lett. A*, vol. 176, pp. 254–258, May 1993.
- [6] X. Baie, J. Colinge, V. Bayot, and E. Grivei, "Quantum-wire effects in thin and narrow SOI MOSFETs," *SOI Conference, 1995. Proceedings., 1995 IEEE International*, pp. 66 – 67, Oct. 1995.
- [7] J. Colinge, X. Baie, V. Bayot, and E. Grivei, "A silicon-on-insulator quantum wire," *Solid-State Electronics*, vol. 39, pp. 49–51, Jan. 1996.
- [8] G. Curatola and G. Iannaccone, "Quantum confinement in silicon-germanium electron waveguides," *Nanotechnology*, vol. 13, no. 3, pp. 267–273, May 2002.
- [9] A. Trellakis and U. Ravaioli, "Directional effects on bound states for trench oxide quantum wires (100)-silicon," *Solid-State Electronics*, pp. 367–371, 2004.
- [10] E. Gnani, S. Reggiani, M. Rudan, and G. Bacarani, "A new approach to the self-consistent solution of the Schroedinger-Poisson equations in nanowire MOSFETs," *Solid-State Device Research conference, 2004. ESSDERC 2004*, pp. 177–180, Sept. 2004.
- [11] E. Pokatilov, V. Fomin, S. Balaban, V. Gladilin, S. Klimin, J. Devreese, W. Magnus, W. Schoenmaker, N. Collaert, M. V. Rossum, and K. D. Meyer, "Distribution of fields and charge carriers in cylindrical nanosize silicon-based metal-oxide-semiconductor structures," *J. of Appl. Phys.*, vol. 85, no. 9, pp. 6625–6631, May 1999.
- [12] D. Jiménez, J. Sáenz, B. Iniguez, J. Suné, L. Marsal, and J. Pallarès, "Unified compact model for the ballistic quantum wire and quantum well metal-oxide-semiconductor field-effect-transistor," *J. Appl. Phys.*, vol. 94, no. 2, pp. 1061–1068, July 2003.
- [13] D. Jiménez, B. Iniguez, J. Suné, L. Marsal, J. Pallarès, J. Roig, and D. Flores, "Continuous analytic I-V model for surrounding-gate mosfets," *Electron Device Letters*, vol. 25, no. 8, pp. 571–573, aug 2004.
- [14] B. Iniguez, D. Jimenez, J. Roig, H. Hamid, L. Marsal, and J. Pallares, "Explicit continuous model for long-channel undoped surrounding gate mosfets," *IEEE Trans. Electron Devices*, vol. 52, no. 8, pp. 1868–1873, Aug. 2005.
- [15] B. Iniguez, T. Fjeldly, A. Lazaro, F. Danneville, and M. Deen, "Compact-modeling solutions for nanoscale double-gate and gate-all-around MOSFETs," *IEEE Trans. Electron Devices*, no. 53, pp. 2128–2141, 2006.
- [16] J. Wang, E. Polizzi, and M. Lundstrom, "A three-dimensional quantum simulation of silicon nanowire transistors," *J. of Appl. Phys.*, vol. 96, no. 4, pp. 2192–2203, aug 2004.
- [17] G. Fiori and G. Iannaccone, "Three-dimensional simulation of one dimensional transport in silicon nanowire transistors," *IEEE Trans. Nanotechnol.*, vol. 6, pp. 524–529, Sept. 2007.
- [18] B. Paul, R. Tu, S. Fujita, M. Okajima, T. Lee, and Y. Nishi, "Theory of ballistic nanotransistors," *IEEE Trans. Electron Devices*, vol. 54, no. 7, pp. 1637–1644, July 2007.
- [19] S. Jin, Y. Park, and H.S.Min, "A three-dimensional simulation of quantum transport in silicon nanowire transistor in presence of electron-phonon interactions," *J. Appl. Phys.*, vol. 99, p. 123719, 2006.
- [20] M. Gilbert, R. Akis, and D. Ferry, "Phonon-assisted ballistic to diffusive crossover in silicon nanowire transistor," *J. Appl. Phys.*, vol. 98, no. 9, p. 094303, Nov. 2005.
- [21] M. Gilbert and S. Banerjee, "Ballistic to diffusive crossover in III-IV nanowire transistors," *IEEE Trans. on Electron Devices*, vol. 54, no. 4, pp. 645–653, Apr. 2007.
- [22] M. Büttiker, "Role of quantum coherence in series resistors," *Phys. Rev. B*, no. 33, pp. 3020–3026, 1986.
- [23] G. Mugnaini and G. Iannaccone, "Physics-based compact models of nanoscale MOSFETs. Part I: Transition from drift-diffusion to ballistic transport," *IEEE Trans. Electron Devices*, vol. 52, no. 8, pp. 1795–1801, Aug. 2005.
- [24] —, "Physics-based compact models of nanoscale MOSFETs. Part II: effects of degeneracy on transport," *IEEE Trans. Electron Devices*, vol. 52, no. 8, pp. 1802–1806, aug 2005.
- [25] —, "Analytical model for nanowire and nanotube transistor covering both dissipative and ballistic transport," *Solid-State Device Research Conference, 2005.*, pp. 213 – 216, Sept. 2005.
- [26] M. Lundstrom, "Elementary scattering theory of the Si mosfet," *IEEE Electron Device Lett.*, vol. 18, no. 7, pp. 361–363, July 1997.
- [27] A. Rahman and M. Lundstrom, "A compact scattering model for the nanoscale double-gate MOSFET," *IEEE Trans. Electron Devices*, vol. 49, pp. 481–489, Mar. 2002.
- [28] J. Lopez-Villanueva, P. Cartujo-Cassinello, F. Gamiz, J. Banqueri, and A. Palma, "Effects of the inversion layer centroid on the performance of double-gate MOSFET's," *IEEE Trans. Electron Devices*, vol. 47, no. 1, pp. 141–146, jan 2000.
- [29] M. Goano, "Algorithm 745: Computation of the complete and incomplete Fermi-Dirac integral," *ACM Trans. on Math. Soft.*, vol. 21, no. 3, pp. 221–232, Sept. 1995.
- [30] J. Roldan, A. Godoy, F. Gamiz, and M. Balaguer, "Modeling the centroid and unversion charge in cylindrical surroundig gate MOSFETs, including quantum effects," *IEEE Trans. Electron Devices*, vol. 55, no. 1, pp. 411–416, Jan. 2008.
- [31] C. Crowell and M. Hafizi, "Current transport over parabolic potential barriers in semiconductor devices," *IEEE Trans. Electron Devices*, vol. 35, no. 7, pp. 1087–1095, jul 1988.
- [32] J. Watling, L. Yang, M. Borici, R. Wilkins, A. Asenov, J. Barker, and S. Roy, "The impact of interface roughness scattering and degeneracy in relaxed and strained Si n-channel MOSFETs," *Solid-State Electronics*, vol. 48, no. 8, pp. 1337–1346, aug 2004.
- [33] C. Liang, X. Shi, and J. Yang, "The variational closed-form formulae for the capacitance of one type of conformal coaxial lines," *Progress In Electromagnetics Research*, no. 45, p. 277289, 2004.
- [34] G. Curatola and G. Iannaccone, "NANOTCAD2D: Two-dimensional code for the simulation of nanoelectronic devices and structures," *Comput. Mater. Sci.*, vol. 28, no. 7, pp. 342–352, July 2003.
- [35] K. Natori, "Ballistic/quasi-ballistic transport in nanoscale transistor," *Appl. Surf. Sci.*, vol. 254, pp. 6194–6198, 2008.
- [36] T. L. Chen and G. Gildenblat, "Symmetric bulk charge linearisation in charge-sheet MOSFET model," *Electronics Letters*, vol. 37, no. 12, pp. 791–793, June 2001.
- [37] X. Gu and G. Gildenblat, "Charge-sheet MOSFET model with surface degeneracy and freezeout," in *International Semiconductor Device Research Symposium*, Dec. 2001, pp. 102–105.